中國機械工程學刊第四十三卷第五期第 421~429 頁(民國一百一十一年)
Journal of the Chinese Society of Mechanical Engineers, Vol.43, No.5, pp.421~429 (2022)

DC and Quasi-DC Acceleration Observation for Servosystems with Piezoelectric Accelerometers

Yu-Sheng Lu* and Po-Chen Lee**

Keywords：acceleration, observer, piezoelectric accelerometer, servo system.

ABSTRACT

This paper presents two observers, which combine a piezoelectric accelerometer with a positional sensor that commonly exists in a servo system. The piezoelectric accelerometers have wide measurement bandwidth but cannot measure an acceleration's dc and quasi-dc components. The proposed observers can estimate dc and quasi-dc components of an acceleration, avoiding the piezoelectric accelerometers' drawback. In contrast to commonly used capacitive accelerometers, the proposed observers can produce wide dynamic bandwidth owing to the use of a piezoelectric accelerometer. Compared with existing acceleration observers, the proposed observers do not require a plant's model and are thus completely insensitive to model uncertainties. Moreover, the proposed observers do not directly differentiate the positional signal twice with respect to time and are thus more immune to positional sensor noise. The proposed observers are experimentally applied to a linear motion stage to investigate applicability and feasibility of the proposed schemes.

INTRODUCTION

Nowadays there are abundant applications of acceleration information to servo control systems. De Jager (1994) proposed acceleration-assisted tracking control, which used a measured acceleration signal for feedback control. The conclusions of this study (De Jager, 1994) are that acceleration signals can be employed to efficiently improve tracking performance, and that the use of acceleration feedback is more effective than increasing the sampling frequency. Tian et al. (2016) applied an acceleration signal to a charge-coupled device-based fast steering mirror control system, which forms an acceleration feedback loop to achieve a high control bandwidth. In the literature (Xu et al., 2000; Hamandi et al., 2020), acceleration signals were added to feedback control laws for controlling a robotic arm and quadrotor aerial vehicles, respectively.

Acceleration signals can further be used to estimate unknown disturbances in servo systems, such as the time-delay control/estimation method (Youcef-Toumi and Ito, 1990) and acceleration-based disturbance observer (ADOB) (Deng et al., 2016). Moreover, acceleration signals can be used to estimate motion speed. Gees (1996) proposed an accelerometer-assisted velocity estimator and applied it to linear-drive machine tool axes. Jeon and Tomizuka (2007) used a kinematic Kalman filter that adds an acceleration signal to velocity estimation. Zhu and Lamarche (2007) used an auxiliary filter that fuses an accelerometer with a positional sensor for velocity estimation. Lu and Liu (2015) designed an acceleration-assisted speed estimator and applied it to a servo system. Lu and Lee (2017) introduced an acceleration signal into traditional Tracking Differentiator as well as a differentiator using Super-Twisting Algorithm for performance enhancement. The study (Xia et al., 2020) proposed a method to estimate a velocity signal from gap and acceleration sensors for magnetic levitation systems. These previous studies showed that velocity feedback can improve a system's transient response while the acceleration signal can effectively facilitate velocity estimation in a servo system.

Another application of acceleration signals to servo systems is the estimation of contact force with an environment. By installing an accelerometer on a robot arm and using the acceleration measurement, the force of the mechanical arm in contact with an environment is estimated using the time-delay estimation method (Youcef-Toumi and Ito, 1990), so that force-sensorless impedance control presented in the literature (Jin et al., 2008; Kang et al., 2009; Jeong et al., 2011) can be achieved. The studies (Mitsantisuk et al., 2011; Phuong et al., 2011) combined accelerometers with the disturbance observer (DOB) and Kalman filter and proposed a

Paper Received August, 2019. Revised January, 2021..Accepted January, 2021. Author for Correspondence: Yu-Sheng Lu.

* *Professor, Department of Mechatronic Engineering, National Taiwan Normal University, Taipei 106, Taiwan, ROC.*

** *Graduate Student, Department of Mechatronic Engineering, National Taiwan Normal University, Taipei 106, Taiwan, ROC.*

force estimation method for bilateral control and sensorless force control. The study (Yokoyama et al., 2021) applied acceleration signals to estimating an external force in linear series elastic actuators.

In the study (Abir et al., 2016), an acceleration signal is used to measure the dynamic displacement of a motion system. In summary, an acceleration signal can be directly used in a control law to improve trajectory tracking performance. It can also be used to estimate an uncertain disturbance or a contact force, demonstrating the importance of acceleration signals to servo systems. However, "*an accurate and clean acceleration signal is needed to be useful, so a high accuracy sensor is necessary and filters should be used to increase the signal-to-noise ratio, without adding too much phase shift.*" (De Jager, 1994)

RELATED WORKS

The method of obtaining acceleration signals can be roughly divided into two categories: indirect estimation methods and direct measurement methods. Without using an accelerometer, the indirect estimation methods usually only require a positional sensor. For example, the study (Han et al., 2007) combined a Newton predictor with a Kalman filter and proposed an acceleration estimator for acceleration feedback control of a two-axis robot arm. Such indirect estimation methods are usually limited by the positional sensor's resolution, and their performance needs to be improved.

Direct measurement methods use accelerometers to sense acceleration. According to different sensing principles, the accelerometers can be categorized as piezo-resistive, piezoelectric, capacitive, thermal, etc. (Lu et al., 2018). The piezoelectric and capacitive accelerometers are the most popular in the current market. Piezoelectric accelerometers have many advantages, including high rigidity, high sensitivity, and fast dynamic response. Hence, they are often used in vibration measurement (Tsai et al., 2017). However, its price is relatively expensive, and it cannot sense dc and quasi-dc acceleration. That is, its low frequency response is inadequate. Capacitive accelerometers benefit from the recent advance of microelectromechanical systems (MEMS) technology, which integrates mechanical and electronic elements in an extremely small size. The capacitive accelerometers can sense dc and quasi-dc acceleration with high sensitivity. However, its frequency response has a small bandwidth, and the signal-to-noise ratio performance is relatively poor (Lu et al., 2018).

As previously described, although capacitive accelerometers can sense dc and quasi-dc acceleration, they have the disadvantage of limited dynamic responses. On the other hand, piezoelectric accelerometers have a high bandwidth but cannot measure dc and quasi-dc acceleration. In the study (Lu et al., 2018), an integrated accelerometer was proposed, which can measure dc and quasi-dc acceleration and also have high dynamic bandwidth. The concept is as follows: the acceleration signal by a capacitive accelerometer is processed by a low-pass filter, whose cut-off frequency is higher than the lower-band edge frequency of a piezoelectric accelerometer. At the same time, the piezoelectric accelerometer's output signal is filtered by a high-pass filter, whose cutoff frequency is less than the cutoff frequency of the capacitive accelerometer, and then these two signals are combined to obtain a complete acceleration signal. However, its disadvantage is that both capacitive and piezoelectric accelerometers are needed simultaneously. The study (Katsura et al., 2008) proposed the so-called PAIDO estimation architecture, which uses a piezoelectric accelerometer and a positional sensor.

This paper introduces a piezoelectric accelerometer's mathematical model and proposes observers that fuse the piezoelectric accelerometer with a positional sensor. Compared to previous integrated accelerometers (Lu et al., 2018), the proposed observers do not require the use of a capacitive accelerometer. Compared with the PAIDO method (Katsura et al., 2008), the proposed observers do not directly differentiate the positional signal twice, producing a better acceleration estimation. In this paper, the proposed observers are applied to a linear motion platform, and the PAIDO is also implemented for performance comparisons.

REVISIT OF THE PAIDO

The study (Katsura et al., 2008) proposed the so-called PAIDO estimation architecture that fuses accelerometer data with positional data. In the PAIDO, there are two intermediate acceleration signals: one is a twice-differentiated positional signal, and the other is the output of a piezoelectric accelerometer. The PAIDO differentiates the positional signal twice with respect to time, fuses two intermediate acceleration signals with complementary filters, and obtains the final acceleration estimate.

Figure 1 shows the PAIDO's structure, where x denotes the positional signal, a_{p} is the piezoelectric accelerometer's output, a_{d} is an acceleration estimate of the PAIDO, ω_{pd} is a cutoff frequency of a low-pass filter, and ω_{dis} is a complementary filter's parameter. The PAIDO differentiates the positional signal (x) twice, uses the complementary filter to reserve its low-frequency part, combines the high-frequency part of the piezoelectric accelerometer's output (a_{p}), and finally obtains its acceleration estimate. Since the piezoelectric accelerometer cannot measure *dc* and quasi-*dc* signals, this method uses the second derivative of a positional signal to estimate the *dc* and quasi-*dc* acceleration, which is then combined with the piezoelectric accelerometer's measure, obtaining a complete acceleration estimate.

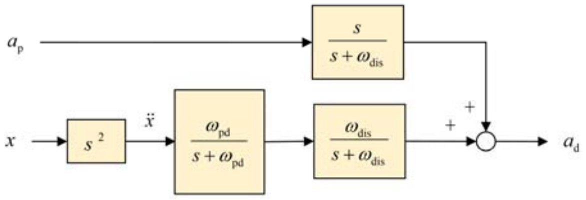

Fig. 1. Structure of the PAIDO.

DESIGN OF AN OBSERVER

First, define the variable, $v = \dot{x}$, as the velocity whereas $a = \dot{v}$ denotes the true acceleration. Since a piezoelectric accelerometer only measures high-frequency acceleration components, a first-order high-pass model is used as its transfer function, namely:

$$\frac{a_p(s)}{a(s)} = \frac{s}{s+\omega_c}, \tag{1}$$

where $a_p(s)$ and $a(s)$ denote the Laplace transforms of $a_p(t)$ and $a(t)$, respectively, and ω_c denotes the lower cutoff frequency of a piezoelectric accelerometer and can be obtained from specifications of a piezoelectric accelerometer. Rearrange Eq. (1) as:

$$a(s) = \frac{s+\omega_c}{s} a_p(s) = a_p(s) + \zeta(s), \tag{2}$$

where the variable $\zeta(s) = \frac{\omega_c}{s} a_p(s)$. The relation among $x(t)$, $v(t)$, and $\zeta(t)$ can be written as:

$$\begin{aligned} &\dot{x}(t) = v(t), \\ &\dot{v}(t) = a(t) = \zeta(t) + a_p(t), \\ &\dot{\zeta}(t) = \omega_c a_p(t), \\ &z(t) = x(t), \end{aligned} \tag{3}$$

where $z(t)$ denotes a measurable output in addition to $a_p(t)$. Define a state vector $\mathbf{q} = \begin{bmatrix} x & v & \zeta \end{bmatrix}^T$, and rewrite Eq. (3) in state-space representation as:

$$\dot{\mathbf{q}} = \mathbf{F}\,\mathbf{q} + \mathbf{G}\,a_p, \qquad z = \mathbf{H}\,\mathbf{q}, \tag{4}$$

where $a_p(t)$ is considered an input to system (4),

$$\mathbf{F} = \begin{bmatrix} 0 & 1 & 0 \\ 0 & 0 & 1 \\ 0 & 0 & 0 \end{bmatrix}, \ \mathbf{G} = \begin{bmatrix} 0 \\ 1 \\ \omega_c \end{bmatrix}, \text{and } \mathbf{H} = \begin{bmatrix} 1 & 0 & 0 \end{bmatrix}.$$

Since the rank of the observability matrix of system (4) is 3, system (4) is completely observable. Define the observer's state vector as $\mathbf{q}_o = \begin{bmatrix} x_o & v_o & \zeta_o \end{bmatrix}^T$. Let the proposed observer be described by:

$$\begin{aligned} &\dot{\mathbf{q}}_o = \mathbf{F}\,\mathbf{q}_o + \mathbf{G}\,a_p + \mathbf{K}\left(x - z_o\right), \\ &z_o = \mathbf{H}\,\mathbf{q}_o, \end{aligned} \tag{5}$$

where z_o is an output estimate, and $\mathbf{K} = \begin{bmatrix} k_1 & k_2 & k_3 \end{bmatrix}^T$ denotes a constant vector of observer gains. Since system (4) is fully observable, the designer can assign the observer gains using the pole-assignment method, placing the poles of the observer at any desired locations in the *s*-plane. Define a_o as the acceleration estimate by the observer. According to Eq. (2), the acceleration estimate produced by the observer should be:

$$a_o = \zeta_o + a_p. \tag{6}$$

Compared with the PAIDO, the proposed observer does not explicitly differentiate the positional signal twice with respect to time, being more immune to positional noise.

DESIGN OF AN EXTENDED OBSERVER

Although the observer (5) does not explicitly differentiate the positional signal, it is unable to attenuate measurement noise of a piezoelectric accelerometer, as shown by Eq. (6). To attenuate the measurement noise in a_p, an extended observer is devised as follows. Rearrange Eq. (1) as:

$$a_p(s) = \frac{s}{s+\omega_c} a(s) = a(s) - \zeta(s), \tag{7}$$

where the variable $\zeta(s) = \frac{\omega_c}{s+\omega_c} a(s)$. Assume that $\dot{a}(t) = 0$, and express the relationships among $x(t)$, $v(t)$, $a(t)$, and $\zeta(t)$ as follows:

$$\begin{aligned} &\dot{x}(t) = v(t), \\ &\dot{v}(t) = a(t), \\ &\dot{a}(t) = 0, \\ &\dot{\zeta}(t) = \omega_c a(t) - \omega_c \zeta(t), \\ &z_1(t) = x(t), \\ &z_2(t) = a_p(t) = a(t) - \zeta(t), \end{aligned} \tag{8}$$

where $z_1(t)$ and $z_2(t)$ are measurable variables. Define a state vector, $\mathbf{q}_e = \begin{bmatrix} x & v & a & \zeta \end{bmatrix}^T$, and an output vector, $\mathbf{z}_e = \begin{bmatrix} z_1 & z_2 \end{bmatrix}^T$. Rewrite Eq. (8) in state-space representation as:

$$\dot{\mathbf{q}}_e = \mathbf{F}_e\,\mathbf{q}_e, \qquad \mathbf{z}_e = \mathbf{H}_e\,\mathbf{q}_e, \tag{9}$$

$$\mathbf{F}_e = \begin{bmatrix} 0 & 1 & 0 & 0 \\ 0 & 0 & 1 & 0 \\ 0 & 0 & 0 & 0 \\ 0 & 0 & \omega_c & -\omega_c \end{bmatrix}, \quad \mathbf{H}_e = \begin{bmatrix} 1 & 0 & 0 & 0 \\ 0 & 0 & 1 & -1 \end{bmatrix}.$$

Since the observability matrix of system (9) is of full rank, system (9) is fully observable. Define the state vector of the extended observer as $\mathbf{q}_{oe} = \begin{bmatrix} x_{oe} & v_{oe} & a_{oe} & \zeta_{oe} \end{bmatrix}^T$, where a_{oe} denotes the acceleration estimate by the extended observer. Design the proposed extended observer to be:

$$\dot{\mathbf{q}}_{oe} = \mathbf{F}_e \mathbf{x}_{oe} + \mathbf{K}_e \left(\begin{bmatrix} x \\ a_p \end{bmatrix} - \mathbf{z}_{oe} \right), \tag{10}$$

$$\mathbf{z}_{oe} = \mathbf{H}_e \, \mathbf{q}_{oe},$$

where $\mathbf{z}_{oe}$ is the observer's output vector, and $\mathbf{K}_e = \left[k_{ij} \right]$, $i = 1, 2, 3, 4$, $j = 1, 2$, denotes a vector of observer gains. Since system (9) is fully observable, the designer can determine the observer gains using the pole-assignment method and arbitrarily place the poles of the extended observer.

EXPERIMENTAL SYSTEM

The acceleration observation is applied to a linear motion platform with single degree of freedom. Figure 2 shows the structure of the linear stage system, in which the motor is a rotating permanent magnet ac motor, and a ball screw converts rotational motion into linear motion of payload. The platform's sensing part contains an optical linear scale for measuring the payload's displacement. A- and B-phase signals from the optical scale are fed back to an FPGA, and the displacement is counted by the FPGA. The payload's acceleration is sensed by both capacitive and piezoelectric accelerometers for performance comparisons.

The DSP reads the displacement count of the payload and the acceleration signals of the two accelerometers from the FPGA, executes trajectory tracking control laws and acceleration observation algorithms, and passes control efforts through a DAC to a current converter that drives the motor so that the payload can track a reference command.

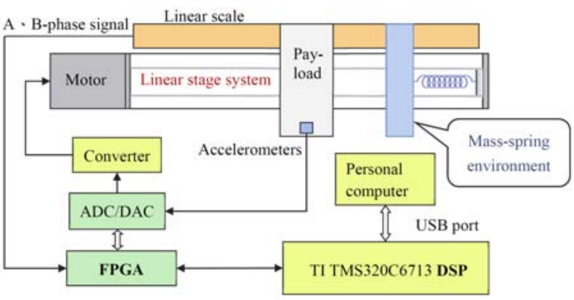

Fig. 2. Structure of the linear stage system.

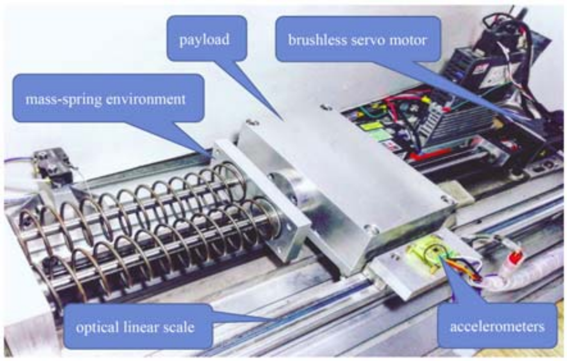

Fig. 3. Photo of the linear stage system.

Figure 3 shows a photo of the experimental linear motion platform. The motor is a Mitsubishi HF-MP43 motor. The linear module, consisting of a ball screw, is of model KK6010P-600A1-F0. Payload is placed on the linear module, and the slider of an optical linear scale is connected to the payload. The optical linear scale of Carmar's WTB5-0600MM is used to sense the payload's displacement. The capacitive accelerometer is Analog Devices Inc.'s ADXL325 whereas the piezoelectric accelerometer is PCB Piezotronics Inc.'s ICP-form accelerometer of model 333B50. A circuit board is added to the slider of the optical linear scale and contains a constant current circuit, required by the piezoelectric accelerometer, and some other analog circuits.

To measure the plant's frequency response, an NI's PXI-4461 Dynamic Signal Analyzer (DSA) is used. The DSA outputs a swept sine whose frequency increases from 1 rad/s to 100 rad/s. The swept sine is forwarded to the motor drive as a torque command. As previously mentioned, the A- and B-phase signals from the optical scale are sent to the FPGA, and the FPGA does the position counting. The DSP reads this position count to determine the payload's displacement. A velocity signal is then obtained by taking the backward difference of the positional signal and passing through a first-order low-pass filter with a cutoff frequency of 50 Hz. During a frequency-response measurement, the DSP outputs a voltage proportional to the load velocity through the DAC to the DSA. After performing curve-fitting with Matlab, a mathematical model of the linear motion platform is found as: $\ddot{x} + \beta\,\dot{x} = \gamma\,u$, where the system input, u, is a force-producing command, and system parameters $\beta = 0.8234$ and $\gamma = 1479$. Moreover, by measuring the output force of the linear motion platform by a load cell, a static relation between the DAC output (i.e., the input to the plant) and the plant's output force is obtained. This result, together with the previously identified parameter values, gives:

$$M\,\ddot{x} + B\dot{x} = G\left(u + d\right), \tag{11}$$

where the mass $M = 28.13$ (kg), the viscous damping coefficient $B = 23.16$ (Ns/m), the input gain $G = 41.6\ (\mathrm{N/V})$, and d denotes an unknown disturbance.

EXPERIMENTAL RESULTS

To evaluate the quality of various acceleration signals, position control of the payload is performed with an ADOB. The ADOB receives different acceleration signals and generates respective disturbance estimates. The disturbance estimate produced by the ADOB is fed back to the control system for disturbance compensation. The quality of various acceleration signals is then evaluated based on their effectiveness in disturbance compensation. An effective disturbance compensation can reduce positional tracking error. Therefore, with the ADOB, the positional tracking error is used to evaluate the quality of various acceleration signals.

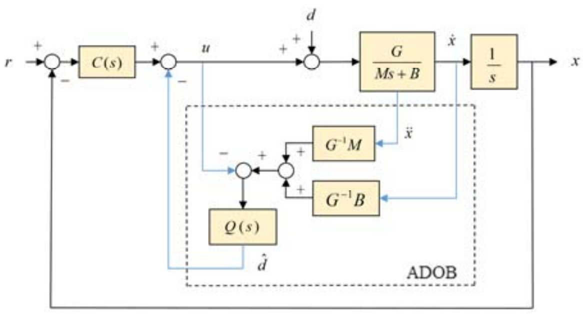

Fig. 4. Control system structure.

Controller/Observer Design

As shown in Figs. 2 and 3, a mass-spring environment is installed on the platform to have the payload in contact with the environment, the environment applies a disturbance to the payload, and the ADOB performs disturbance compensation. Figure 4 depicts the structure of the ADOB-based control system, in which r denotes a reference command, $C(s)$ represents a nominal controller, $\hat{d}$ is a disturbance estimate, and $Q(s)$ denotes a low-pass filter. Define the positional tracking error $e = x - r$. According to model (11), the controller is designed as:

$$u = G^{-1}\left\{ B\dot{x} + M\left[\ddot{r} - M_{\mathrm{t}}^{-1}\left(B_{\mathrm{t}}\dot{e} + K_{\mathrm{t}}e\right)\right]\right\} - \hat{d}\ , \quad (12)$$

where M_{t}, B_{t} and K_{t} are the target mass, damping and spring coefficients, respectively. As shown in Fig. 4, this study constructs an ADOB, where $Q(s)$ is a first-order low-pass filter having a corner frequency of 15 Hz. The acceleration signal to the ADOB can be generated by two accelerometers or three acceleration observers. The two accelerometers are capacitive and piezoelectric accelerometers, whose outputs are respectively denoted as a_{c} and a_{p}. The three observers are the PAIDO, the proposed observer, and the proposed extended observer, whose outputs are respectively denoted as a_{d}, a_{o}, and a_{oe}. If there is a clean, accurate acceleration signal, the ADOB can effectively counteract external disturbance, yielding excellent tracking performance. This study uses the ADOB to evaluate the pros and cons of various acceleration signals according to positional tracking performance.

In following experiments, let the controller parameters $M_{\mathrm{t}} = M$, $B_{\mathrm{t}} = 2M\omega_{\mathrm{n}}$, and $K_{\mathrm{t}} = M\omega_{\mathrm{n}}^2$, where $\omega_{\mathrm{n}} = 25$. The lower-band edge frequency of the piezoelectric accelerometer is $\omega_c = 0.3\pi$ (rad/s). The parameters of the proposed observer is set such that the observer poles equal -200π and $-200\pi(1 \pm \mathrm{j})/\sqrt{2}$. Likewise, the poles of the proposed extended observer are set to double poles of -200π and $-200\pi(1 \pm \mathrm{j})/\sqrt{2}$. The reference command to be used is a minimum-jerk command:

$$\begin{aligned} r = {} & \ell\left[10t^3 - 15t^4 + 6t^5\right]\ \left(H(t) - H(t-1)\right) + \\ & \ell\left[1 + 10(t-1)^3 - 15(t-1)^4 + 6(t-1)^5\right]\ \left(H(t-1) - H(t-2)\right) + \\ & \ell\left[1 + 10(3-t)^3 - 15(3-t)^4 + 6(3-t)^5\right]\ \left(H(t-2) - H(t-3)\right) + \\ & \ell\left[10(4-\tau)^3 - 15(4-\tau)^4 + 6(4-\tau)^5\right]\ \left(H(t-3) - H(t-4)\right), \end{aligned}$$

where $\ell = 30$ (mm), and $H(\cdot)$ represents the unit-step function. Since the mass-spring environment is initially at the position of 30 (mm), the payload will collide with the environment at this position. When the payload follows the minimum-jerk command, it will be in contact with the environment from 1 to 3 s. To evaluate tracking performance, define performance indices of integral of absolute error (*IAE*) and chatter index (*CI*) as follows:

$$IAE_e = \int_0^{t_{\mathrm{f}}} \left|e(t)\right| dt, \qquad CI_e = \frac{1}{t_{\mathrm{f}}}\int_0^{t_{\mathrm{f}}} \left|e(t) - \overline{e}(t)\right| dt,$$

$$CI_u = \frac{1}{t_{\mathrm{f}}}\int_0^{t_{\mathrm{f}}} \left|u(t) - \overline{u}(t)\right| dt, \quad (13)$$

where $\overline{e}(t)$ is a filtered tracking error, and $\overline{u}(t)$ is a filtered control effort. Concerning the filtering, a second-order filter with a corner frequency of 50 rad/s is designed by Matlab's *butter* function, and the filter is offline realized using the *filtfilt* function of Matlab to achieve zero-phase filtering. The parameter t_{f} in Eq. (13) denotes the final time, which is 4.00488 s with the minimum-jerk command. The higher *CI* of a signal is, the more high-frequency components the signal has, and the more uneven the signal is. Hence, the performance index, *CI*, is utilized to indicate high-frequency amounts of a signal. In order to make the experimental results reliable, each response curve shown in subsequent figures is the average of ten consecutive experimental results.

Performance Comparison with Accelerometers

Without using an ADOB, Figs. 5 and 6 respectively show tracking responses and acceleration signals subject to the minimum-jerk reference. As seen from Fig. 6, a_p and a_c have similar amounts of oscillations when they are not fed back for disturbance compensation. Subsequently, use an ADOB with different acceleration signals for disturbance compensation to compare the quality of various acceleration signals. Subject to the minimum-jerk reference, Figs. 7 and 8 respectively show error responses and acceleration signals for disturbance compensation. Although a_p and a_c have similar amounts of oscillations as shown in Fig. 6, it is seen from Fig. 8 that with disturbance compensation using the ADOB, a_c has larger oscillations than a_p. Correspondingly, as seen from Fig. 7, the capacitive accelerometer makes control efforts noisier. Table 1 lists performance indices for these system responses, showing that the extended observer produces smaller output errors and also reduces high-frequency components of the outputs and control efforts. That is, compared with the two accelerometers, the extended observer leads to the smoothest control efforts and also achieve the minimum output error.

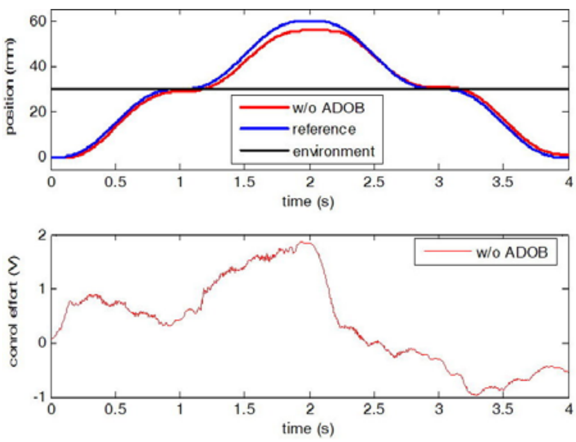

Fig. 5. Tracking response using the nominal control without an ADOB.

Table 1. Performance indices for minimum-jerk responses.

	IAE_e(mm·s)	CI_e(mm)	CI_u(V)
a_p	0.4146	0.0024	0.0314
a_c	0.4046	0.0042	0.0791
a_{oe}	**0.3079**	**0.0022**	**0.0256**

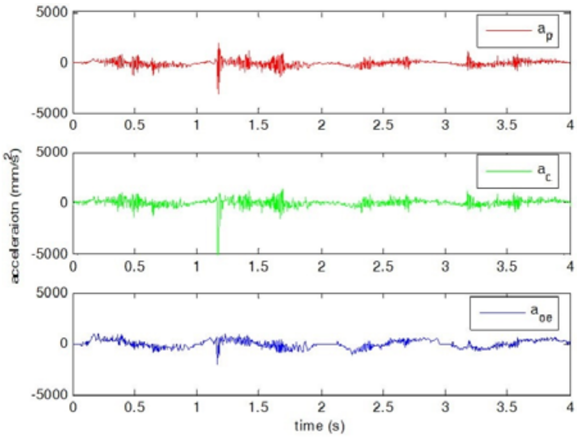

Fig. 6. Acceleration signals during the tracking control without an ADOB.

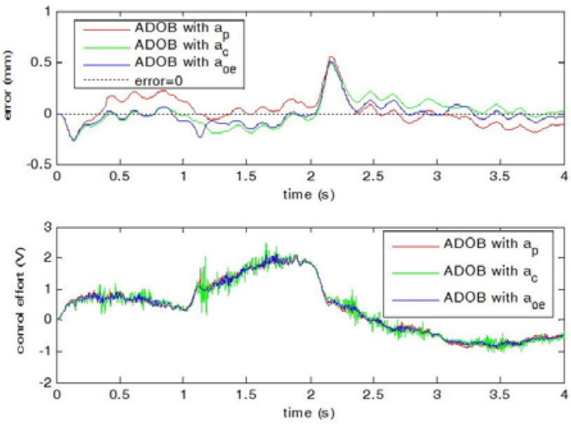

Fig. 7. Tracking responses with an ADOB.

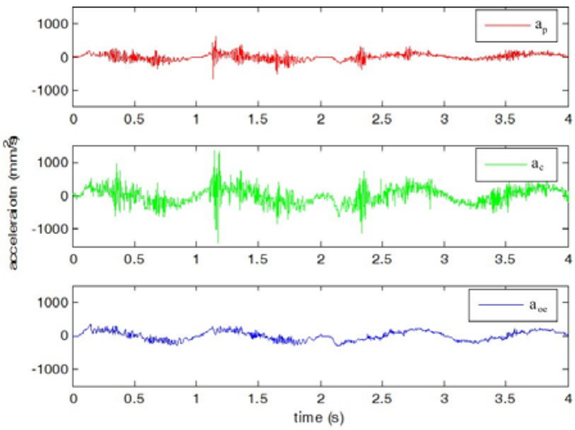

Fig. 8. Acceleration signals during the tracking control with an ADOB.

Parameter Tuning for the PAIDO

The reference (Katsura et al., 2008) proposes the so-called PAIDO estimation scheme, whose structure is shown in Fig. 1. In the PAIDO, there are two parameters, ω_{pd} and ω_{dis}, which needs to be determined. According to the literature (Katsura et al., 2008), choose $\omega_{pd} = 3000$. Various values of ω_{dis} are tested, and the optimal value of ω_{dis} is determined in terms of performance indices. Table 2 lists performance indices of the PAIDO with different values of ω_{dis} subject to the minimum-jerk command. It is seen that when ω_{dis} is reduced, the corresponding CI will also decrease, indicating that high-frequency components of the signal are reduced and that the signal is smoother. However, the value of IAE_e does not have the same trend. It is seen from Table 2 that the error index value is the smallest when $\omega_{\text{dis}} = 30\pi$. Hence, $\omega_{\text{dis}} = 30\pi$ is set in subsequent comparison experiments.

Table 2. PAIDO's performance indices for minimum-jerk responses.

	IAE_e(mm·s)	CI_e(mm)	CI_u(V)
$\omega_{\text{dis}}=50\pi$	0.4221	0.0034	0.0569
$\omega_{\text{dis}}=40\pi$	0.4118	0.0033	0.0561
$\omega_{\text{dis}}=30\pi$	**0.3999**	0.0032	0.0552
$\omega_{\text{dis}}=20\pi$	0.4210	0.0032	0.0549
$\omega_{\text{dis}}=10\pi$	0.4239	0.0030	0.0512

Comparison of Acceleration Estimators

In subsequent experiments, three acceleration estimates, a_{d}, a_{o} and a_{oe}, are individually passed to the ADOB for disturbance compensation. The acceleration observers are also evaluated according to positional dynamic responses of the platform. Figures 9 and 10 respectively show error responses and acceleration estimates for the platform subject to the minimum-jerk reference. It can be seen from Fig. 9 that the PAIDO produces larger high-frequency components in the control efforts. Likewise, Fig. 10 shows that a_{d} has greater high-frequency oscillations than both a_{o} and a_{oe}. Table 3 lists performance indices subject to the minimum-jerk reference, showing that the proposed observer that produces a_{o} is slightly better than the PAIDO. Moreover, the proposed extended observer is the best among these three acceleration observers. That is, the extended observer can achieve the minimum tracking error with the smoothest control efforts.

Table 3. Performance indices for minimum-jerk responses.

	IAE_e(mm·s)	CI_e(mm)	CI_u(V)
a_{oe}	**0.3079**	**0.0022**	**0.0256**
a_{d}	0.3999	0.0032	0.0552
a_{o}	0.3432	0.0025	0.0501

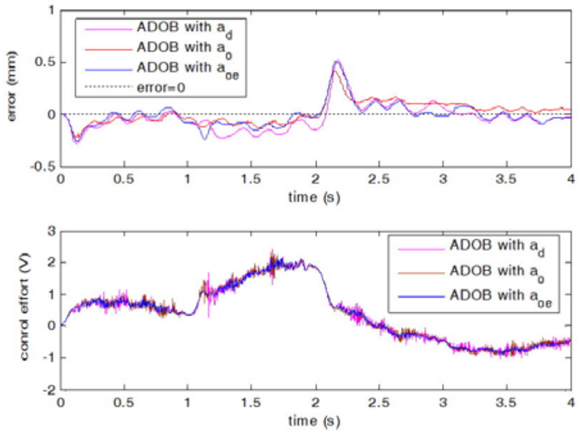

Fig. 9. Tracking response with an ADOB.

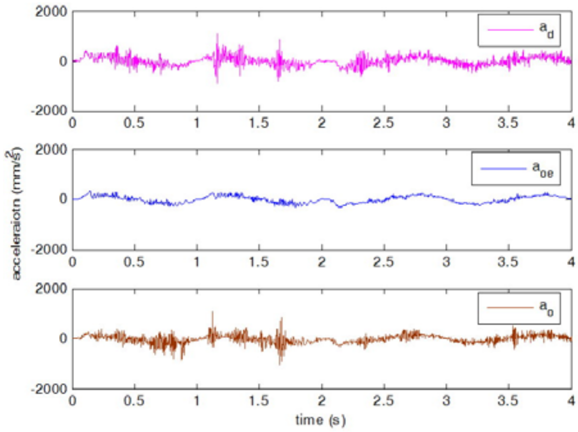

Fig. 10. Acceleration signals during the tracking control with an ADOB.

CONCLUSIONS

Piezoelectric accelerometers have excellent high-frequency dynamics but cannot measure *dc* and quasi-*dc* signals, so they cannot be directly applied to servo systems. To compensate for low-frequency responses of piezoelectric accelerometers, this paper proposes two observers that utilize positional information. Compared with the PAIDO estimation scheme, the observers proposed in this paper do not directly differentiate a positional signal twice, being less influenced by high-frequency noise of the positional signal. Moreover, by introducing an additional state variable into the observer, the extended observer can further diminish high-frequency acceleration noise. Experimental results confirm the effectiveness of the proposed observers. In addition, the proposed observers can produce estimates of velocity and position, which can be used in feedback controllers to further improve system performance.

ACKNOWLEDGMENT

This work was supported by the Ministry of Science and Technology, R.O.C., under grant number MOST 107-2221-E-003-021.

REFERENCES

Abir, J., Longo, S., Morantz, P., and Shore, P., "Optimized Estimator for Real-Time Dynamic Displacement Measurement Using Accelerometers," *Mechatronics*, Vol. 39, pp. 1–11 (2016).

De Jager, B., "Acceleration Assisted Tracking Control," *IEEE Control Systems Magazine*, Vol. 14, No. 5, pp. 20–27 (1994).

Deng, C., Mao, Y., and Ren, G., "MEMS Inertial Sensors-Based Multi-Loop Control Enhanced by Disturbance Observation and Compensation for Fast Steering Mirror System," *Sensors*, Vol. 16, pp. 1920–1931 (2016).

Gees, A., *Accelerometer-Enhanced Speed Estimation for Linear-Drive Machine Tool Axes*. Ph.D. dissertation, Lausanne, Switzerland (1996).

Han, J.D., He, Y.Q., and Xu, W.L., "Angular Acceleration Estimation and Feedback Control: An Experimental Investigation," *Mechatronics*, Vol. 17, No. 9, pp. 524–532 (2007).

Hamandi, M., Tognon, M., and Franchi, A., "Direct Acceleration Feedback Control of Quadrotor Aerial Vehicles," *Proc. 2020 IEEE International Conference on Robotics and Automation*, Paris, France, pp. 5335–5341 (2020).

Jeon, S., and Tomizuka, M., "Benefits of Acceleration Measurement in Velocity Estimation and Motion Control," *Control Eng. Pract.*, Vol. 15, pp. 325–332 (2007).

Jeong, J.W., Chang, P.H., and Park, K.B., "Sensorless and Modeless Estimation of External Force Using Time Delay Estimation: Application to Impedance Control," *J. Mech. Sci. Technol.*, Vol. 25, pp. 2051–2059 (2011).

Jin, M., Kang, S.H., and Chang, P.H., "Robust Compliant Motion Control of Robot with Nonlinear Friction Using Time-Delay Estimation," *IEEE Trans. Industrial Electronics*, Vol. 55, No. 1, pp. 258–269 (2008).

Kang, S.H., Jin, M., and Chang, P.H., "A Solution to the Accuracy/Robustness Dilemma in Impedance Control," *IEEE/ASME Trans. Mechatronics*, Vol. 14, No. 3, pp. 282–294 (2009).

Katsura, S., Irie, K., and Ohishi, K., "Wideband Force Control by Position Acceleration Integrated Disturbance Observer," *IEEE Trans. Ind. Electron.*, Vol. 55, No. 4, pp. 1699–1706 (2008).

Lu, Y.S., and Lee, C.H., "Experimental Evaluation of Acceleration-Enhanced Velocity Estimation Algorithms Using a Linear Motion Stage," *Journal of the Brazilian Society of Mechanical Sciences and Engineering*, Vol. 39, No. 2, pp. 543–551 (2017).

Lu, Y.S., and Liu, S.H., "The Design and Implementation of an Accelerometer-Assisted Velocity Observer," *ISA Transactions*, Vol. 59, pp. 418–423 (2015).

Lu, Y.S., Wang, H.W., and Liu, S.H., "An Integrated Accelerometer for Dynamic Motion Systems," *Measurement*, Vol. 125, pp. 471–475 (2018).

Mitsantisuk, C., Ohishi, K., Urushihara, S., and Katsura, S., "Kalman Filter-Based Disturbance Observer and its Applications to Sensorless Force Control," *Adv. Robot.*, Vol. 25, nos. 3–4, pp. 335–353 (2011).

Phuong, T.T., Mitsantisuk, C., and Ohishi, K., "Multi-Sensor Fusion in Kalman-Filter for High Performance Force Sensing," *Proc. 2011 IEEE International Conference on Industrial Technology* (*ICIT*), Auburn, AL, pp. 393–398 (2011).

Tian, J., Yang, W., Peng, Z., Tang, T., and Li, Z., "Application of MEMS Accelerometers and Gyroscopes in Fast Steering Mirror Control Systems," *Sensors*, Vol. 16, pp. 440–452 (2016).

Tsai, P.C., Cheng, C.C., and Hwang, Y.C., "On-line Ball Screw Preload Degradation Monitoring Based on Vibration Signals," *Journal of the Chinese Society of Mechanical Engineers*, Vol.38, No.5, pp489–497 (2017).

Xia, W., Long, Z., and Dou, F., "Disturbance Rejection Control Using a Novel Velocity Fusion Estimation Method for Levitation Control Systems," *IEEE Access*, Vol. 8, pp. 173092–173102 (2020).

Xu, W.L., and Han, J.D., "Joint Acceleration Feedback Control for Robots: Analysis, Sensing and Experiments," *Robotics and Computer-Integrated Manufacturing*, Vol. 16, No. 5, pp. 307–320 (2000).

Yokoyama, M., Petrea, R.A.B., and Oboe, R., "External Force Estimation in Linear Series Elastic Actuator Without Load-Side Encoder," *IEEE Trans. Ind. Electron.*, Vol. 68, No. 1, pp. 861–870 (2021).

Youcef-Toumi, K., and Ito, O., "A Time Delay Controller for Systems with Unknown Dynamics," *ASME J. Dyn. Sys. Meas. Control*, Vol. 112, No. 1, pp. 133–42 (1990).

Zhu, W.H., and Lamarche, T., "Velocity Estimation by Using Position and Acceleration Sensors," *IEEE Trans. Ind. Electron.*, Vol. 54, No. 5, pp. 2706–2715 (2007).

具有壓電式加速規的伺服系統直流與準直流加速度觀測

呂有勝　　李柏辰
國立臺灣師範大學機電工程學系

摘 要

本文介紹了兩個觀測器，它們融合了壓電式加速規（piezoelectric accelerometer）與經常存在於伺服系統中的位置感測器。壓電式加速規具有高的測量頻寬，但無法測量直流和準直流加速度。本文所提出的觀測器可以估測直流和準直流加速度，避免壓電式加速規的缺點。與現有的加速度觀測器相比，本文所提出的觀測器不需要受控體的模型，因此對於受控體模型的不確定性完全不敏感。此外，本文所提出的觀測器不會直接將位置訊號微分兩次，因此對於位置訊號的高頻雜訊較不敏感。透過將所提出的觀測器應用於線性運動平台，本文以實驗方式驗證其適用性和可行性。